INDIAN INSTITUTE OF TECHNOLOGY, BOMBAY

Inertial Navigation System

by

Avnish Kumar

A thesis submitted in partial fulfillment for the
B. Tech. Project

under the guidance of
Prof. Hari B. Hablani
DEPARTMENT OF AEROSPACE ENGINEERING

December 2012

"When there is righteousness in the heart, there is beauty in the character,
When there is beauty in the character, there is harmony in the home,
When there is harmony in the home, there is order in the nation,
And when there is order in the nation there is peace in the world."

- A. P. J. Abdul Kalam

INDIAN INSTITUTE OF TECHNOLOGY, BOMBAY

Abstract

Prof. Hari B. Hablani
DEPARTMENT OF AEROSPACE ENGINEERING

B. Tech. Project

by Avnish Kumar

Inertial navigation blended with other navigation aids like GPS, has gained significance due to enhanced navigation and inertial reference performance. The INS, individually can calculate the position of the aircraft without any help from the out- side world. However, a large number of errors are introduced by sensors leading to an unacceptable drift in the output. Hence a GPS is used to aid the INS, using a Kalman filter which helps in estimating the errors in the INS and thus updating position to improved accuracy.
The first part of the report deals with calibrating a tactical grade inertial sensor unit in a Laboratory environment, using a 3-axis turn table. The latter part of the report focuses on the EKF based tight integration of GPS-INS for improved navigator design. The simulation of the calibration as well as the integration of INS and GPS using Kalman filtering has been done using MATLAB.

...

Acknowledgements

I take this opportunity to express my deep appreciation and gratitude to my guide, Prof. Hari B. Hablani for his valuable insights, guidance and patience which got me through the project. I would also like to thank Prof. Arya for his help during my project.

Date: Prof. Hari B. Hablani

Contents

List of Figures

Chapter 1

Introduction

1.1 Inertial Navigation System

1.1.1 Why INS

No matter what type of motion we are involved in it is always critical to know where we are positioned. Throughout tie several different methods and instruments have been used to navigate to a specific location. Using the stars, the sun or special marks on the landscape. Nowadays GPS is the most widespread navigation system. But in certain applications standalone GPS is not a viable solution. In certain areas, e.g. in mountainous surroundings, or indoor application the GPS signal is either not present or very inaccurate because of multi-path interference. Furthermore, navigation using GPS is dependent on the satellites governed by the USA which might not always be accessible during a war situation.

An INS is a navigation system which depends entirely on inertial measurements for navigation. An INS consists of accelerometers which measure the translational acceleration and gyroscopes which measure the angular rotation of the system. This sensor array is called an Inertial Measurement Unit (IMU). Using the measurements from the IMU, the INS can calculate the current attitude, velocity and position of the system starting from some known initial point. This means that INS does not depend on any third party applications, like GPS, and thus will always work regardless of external influences. This makes it suitable for navigation in places where GPS signal is not present or if the signals are being jammed.

When relying only on inertial measurements, however, the accuracy of the INS degrades with time due to measurement inaccuracies. But used in a short time span, INS gives a much higher precision than GPS. This makes INS very suitable for missiles where precision is crucial, but which are only airborne for a few seconds.

1.1.2 Basic operation

An inertial navigation system (INS) is a set of instruments that allow position and velocity of a vehicle to be determined solely from internal measurements. While other navigation systems may make use of external measurements, such as radar ranging, Doppler shifts, or GPS pseudoranges, an INS merely measures the inertial angular rates and forces on the vehicle. For a properly initialized INS, these measurements can be processed to provide a continuous navigation solution.
In order for an INS to navigate, it must be capable of performing four distinct functions[Britting,1971]:

- Define a reference frame
- Measure a specific force
- Have knowledge of the gravitational force
- Time integrate the specific force data to obtain velocity and position data

These functions are performed by the four basic components of any INS: three gyroscopes, three accelerometers, a gravity calculator, and an onboard digital computer used to integrate the equations of motion.
Gyroscopic instruments are used to accomplish the first function. The three gyroscopes (assumed to have a single degree-of-freedom) can either be placed on a gimbaled platform or rigidly attached to the vehicle. If they are placed on a gimbaled platform, they define an inertially non-rotating cartesian frame.
The second function of the INS is performed by devices called accelerometers. The accelerometers are an integral part of either gimbaled or strapdown INS's. The accelerometers are the instruments that actually measure the forces acting on the body. This is accomplished by using three orthogonal accelerometers. Each accelerometer has a proofmass that is constrained to move in one direction. When a force acts on the body, the body accelerates. If the force has a component along a particular accelerometer's input axis, then the proofmass of that accelerometer will deflect. By measuring the deflection of all the proofmasses, the acceleration magnitude and direction can be determined. Unfortunately, the accelerometer measurements also include the effects of the gravitational field. An accelerometer at rest with no external forces acting on it will read 1g down due to gravity. In order to determine the motion of the vehicle, the gravity accelerations must be removed from the accelerometer outputs. The third function of the INS is then required to accurately compensate the accelerometer outputs for the local gravity forces.

The final function of the INS, performed by an onboard navigating computer, is the integration of the measured forces. The data obtained from the accelerometers and gyros is processed, resulting in the accelerations in the inertial frame. These accelerations may then be integrated once to provide velocity information. The velocity information is then integrated once more to provide position information.

1.1.2.1 Gimballed vs Strapdown INS

Two forms of inertial navigation systems are the gimbaled system and the strapdown system. The difference between the two systems is the way in which the instruments are mounted on the vehicle. In gimbaled systems, the instruments maintain their orientation in an inertially nonrotating frame. In strapdown systems, the instruments are rigidly attached to the vehicle and experience the same angular motion as the vehicle.
Strapdown systems have both advantages and disadvantages over gimbaled systems. The greatest advantage of strapdown systems is their smaller size. Current systems are so small that their weight is almost negligible. Also, the power consumption for these small devices is significantly less than that of the gimbaled systems. With these advantages comes the disadvantage of a larger computational burden in computing a navigation solution. The gyro data must now be processed to determine the orientation of the vehicle with respect to an inertial frame. Also, since the instruments are rotating with the vehicle, there will be errors introduced due to angular motion. These angular motion errors are only present in strapdown systems.

1.2 Nomenclature and Mathematical Techniques

The purpose of this topic is to define the notations used throughout this report and some of the fundamental mathematical techniques which are used in deriving some of the subsequent equations.
Scalars are noted with non-bold letters, vectors as lower-case bold letters and matrices as capital bold letters

v=scalar
$\mathbf{r}$=vector
$\mathbf{\Omega}$=matrix

1.2.1 Coordinate Frames and Transformation

To describe the kinematics of the IMU a set of frames and notations must be agreed upon. All frames used in this report will span a three dimensional Euclidean space, consisting of three orthogonal basis vectors. The basis vectors of the b will be denoted by b_x, b_y, b_z with x, y, z being the principal axis of the frame. A vector $\mathbf{r}$ referenced in the b frame will be denoted r^b.
It is often needed to represent a vector in different coordinate frames. It is customary to write these equations in matrix form as

$$\begin{bmatrix} r_x^j \\ r_y^j \\ r_z^j \end{bmatrix} = \begin{bmatrix} \cos(\phi) & \sin(\phi) & 0 \\ -\sin(\phi) & \cos(\phi) & 0 \\ 0 & 0 & 1 \end{bmatrix} \begin{bmatrix} r_x^i \\ r_y^i \\ r_z^i \end{bmatrix}$$

Here, C_i^j is the rotation matrix transforming $\mathbf{r}$ from frame i to frame j. The rotation matrix is also called the Direction Cosine Matrix (DCM).
The DCM's corresponding to rotations around all principal axes are stated here for completeness

$$Rotation\ about\ X\ axis = \begin{bmatrix} 1 & 0 & 0 \\ 0 & \cos(\phi) & \sin(\phi) \\ 0 & -\sin(\phi) & \cos(\phi) \end{bmatrix} \tag{1.1}$$

$$Rotation\ about\ Y\ axis = \begin{bmatrix} \cos(\theta) & 0 & -\sin(\theta) \\ 0 & 1 & 0 \\ \sin(\theta) & 0 & \cos(\cos) \end{bmatrix} \tag{1.2}$$

$$Rotation\ about\ Z\ axis = \begin{bmatrix} \cos(\psi) & \sin(\psi) & 0 \\ -\sin(\psi) & \cos(\psi) & 0 \\ 0 & 0 & 1 \end{bmatrix} \tag{1.3}$$

It is important to note, that the order in which the rotations around the principal are applied are not arbitrary. An X-Y-Z rotation is not in general the same as an Y-X-Z rotation.

1.2.2 Relative Angular Velocity of Frames

When describing the relative angular velocity of two frames, it is necessary to describe both which frames are involved and in which coordinate system the angular velocity is expressed. If e.g. the angular velocity of frame j relative to frame i is expressed in the j'th coordinate system this is written as

$$\boldsymbol{\omega_{ij}^{j}} = \begin{bmatrix} \omega_{ij,x}^{j} & \omega_{ij,y}^{j} & \omega_{ij,z}^{j} \end{bmatrix}^{T}$$

1.2.3 Computed and measured quantities

In order to distinguish between actual measurements from sensors and computed quantities used in the computer, they are denoted differently. A physical vector measured by a sensor is denoted with a tilde and a computed quantity is denoted by a hat:

$$\begin{aligned} \tilde{\omega}_{ij}^{j} &= \text{measured angular velocity} \\ \hat{\omega}_{ik}^{k} &= \text{computed angular velocity} \end{aligned}$$

1.2.4 Skew Symmetric Matrix

Throughout the report, it is sometimes convenient to change between a vector representation and a matrix representation. In doing so, the skew symmetric matrix is introduced. Using the skew symmetric matrix, the cross product of two vectors reduces to doing a matrix multiplication:

$$\mathbf{a}X\mathbf{b} \;=\; \mathbf{A}\mathbf{b} \tag{1.4}$$

where $\mathbf{A}$ is the skew symmetric matrix form of $\mathbf{a}$. The elements in the skew symmetric matrix is as follows:

$$\begin{aligned} \mathbf{a} &= \begin{bmatrix} a_1 & a_2 & a_3 \end{bmatrix}^{T} \\ \mathbf{A} &= \begin{bmatrix} 0 & -a_3 & a_2 \\ a_3 & 0 & a_1 \\ -a_2 & a_1 & 0 \end{bmatrix} \end{aligned} \tag{1.5}$$

1.2.5 Time Derivative of the Direction Cosine Matrix

At time t, the relation of frame i and j is expressed by the DCM $\boldsymbol{C}_i^j(\mathrm{t})$. During the time δt, the i frame is rotated to a new orientation so the DCM is now $\boldsymbol{C}_i^j(\mathrm{t} + \delta\mathrm{t})$.

By definition, the time derivative of a DCM is:

$$\dot{\mathbf{C}}_i^j = \lim_{\Delta t \to 0} \frac{\mathbf{C}_i^j}{\Delta t} = \lim_{\Delta t \to 0} \frac{\mathbf{C}_i^j(t + \Delta t) \; - \; \mathbf{C}_i^j(t)}{\Delta t} \tag{1.6}$$

Using a geometrical interpretation the small angle rotation $\boldsymbol{C}_i^j$(t+Δ t) is the same as $\boldsymbol{C}_i^j(\boldsymbol{I} + \Delta\boldsymbol{\theta}^i)$ where $\Delta\boldsymbol{\theta}^i$ is the skew symmetric matrix related to the small angle rotation of $\boldsymbol{C}_i^j$ from time t to $t + \delta t$. The skew symmetric form is due to the small angle simplifications applied to the cosine and sine parts of the DCM of the generic X-Y-Z transformation . The result is:

$$\Delta\boldsymbol{\theta}^i = \begin{bmatrix} 0 & \Delta\theta_\gamma & -\Delta\theta_\beta \\ -\Delta\theta_\gamma & 0 & \Delta\theta_\alpha \\ \Delta\theta_\beta & -\Delta\theta_\alpha & 0 \end{bmatrix} \tag{1.7}$$

where $\Delta\theta_\alpha$, $\Delta\theta_\beta$, $\Delta\theta_\gamma$ are the small angles that the i frame has been rotated through. Substituting (2.7) in (2.6) yields:

$$\dot{\boldsymbol{C}}_i^j \; = \; \boldsymbol{C}_i^j \lim_{\delta t \to 0} \frac{\Delta\boldsymbol{\theta}^i}{\Delta t} \tag{1.8}$$

Inspecting the part $\frac{\Delta\boldsymbol{\theta}^i}{\Delta t}$ when $\delta t \to 0$ reveals that it is the same as the angular velocity of the i'th frame with respect to the j'th frame and this is denoted as $\boldsymbol{\omega}_{ji}^i$. This vector can be expressed as a skew symmetric matrix:

$$\boldsymbol{\omega}_{ji}^i = \; \boldsymbol{\Omega}_{ji}^i \tag{1.9}$$

where $\boldsymbol{\Omega}_{ji}^i$ is a skew symmetric version of $\boldsymbol{\omega}_{ji}^i$ of the form from (2.7).
The frame of reference can be changed by transforming the matrix under the similarity transform

$$\boldsymbol{\Omega}_{ij}^i \; = \; \boldsymbol{C}_j^i \boldsymbol{\Omega}_{ij}^j \boldsymbol{C}_{\boldsymbol{i}}^{\boldsymbol{j}} \tag{1.10}$$

Using this property, (2.8) can be written as:

$$\dot{\boldsymbol{C}}_i^j \; = \; \boldsymbol{C}_i^j \boldsymbol{\Omega}_{ji}^i \; = \; -\boldsymbol{\Omega}_{ij}^j \boldsymbol{C}_i^j \tag{1.11}$$

1.3 Frame of Reference and Position Determination

Before explaining the principles of INS, it is important to define the coordinate frames used throughout this report as they are essential to the derivation of the INS equations. As mentioned earlier, in order to model the output of the sensors, an inertial reference

frame is needed, i.e. a frame in which there are no forces acting. Ideally, the inertial frame should include all forces exerted on the IMU, but in practice this is impossible, as this would require knowledge about the entire universe.
Fortunately, it can be shown, that as the resolution of most inertial sensors today are limited, an adequate precision of the inertial frame for use in terrestrial inertial navigation systems is one that includes the rotation of the earth but not the revolving of the earth around the sun [Britting, 1971].

1.3.1 Earth-Centered Inertial Frame

In INS applications, the inertial frame i is chosen as an earth-centered inertial frame (ECI) which has origin at the center of the earth, and one axis parallel to the direction of earth rotation. In this report i_y is such an axis. i_z vector is chosen such that it goes through the equator at the longitude where navigation was started. And i_x is such that it completes the right hand coordinate system.

1.3.2 Earth-Centered Earth-Fixed Frame

The ECEF frame is fixed within the Earth and is rotation, and is centered at the earth's centre. The z axis s parallel to and aligned with the Earth's rotation. In the equatorial plane the x axis locates the Greenwich meridian and the y axis completes the right hand system.

1.4 Equation of Motion

Here we develop expressions for the navigation state in terms of the sensed acceleration and angular rates available from the accelerometers and gyros respectively. The resulting differential equations,can be numerically integrated using mathematical techniques developed in the second chapter.

1.4.1 Velocity Equation

The velocity vector v^n in the rotating navigation frame n, is defined in ECEF frame e position vector as

$$\boldsymbol{v}^n \equiv \boldsymbol{C}_e^n \dot{\boldsymbol{r}}^e \tag{1.12}$$

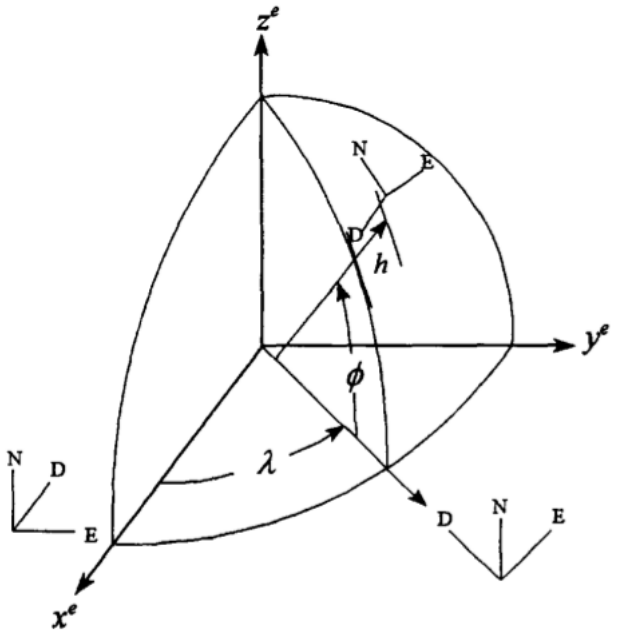

FIGURE 1.1: ECEF frame with z-axis along Earth rotation axis.

The time derivative of this equation is

$$\dot{\boldsymbol{v}}^n \equiv \boldsymbol{C}_e^n \ddot{\boldsymbol{r}}^e + \dot{\boldsymbol{C}}_e^n \dot{\boldsymbol{r}}^e \tag{1.13}$$

Now, the ECEF frame position vectorr^e is related to the non-rotating inertial frame i as

$$\boldsymbol{r}^e = \boldsymbol{C}_i^e \boldsymbol{r}^i \tag{1.14}$$

The time rate change of this equation is

$$\dot{\boldsymbol{r}}^e = \boldsymbol{C}_i^e \dot{\boldsymbol{r}}^i + \dot{\boldsymbol{C}}_i^e \boldsymbol{r}^i \tag{1.15}$$

As we know the time rate change of the direction cosine matrix $\boldsymbol{C}_i^e$ is

$$\dot{\boldsymbol{C}}_i^e = -\boldsymbol{C}_i^e \boldsymbol{\Omega}_{i/e}^i \tag{1.16}$$

which when substituted in (5.4) gives

$$\dot{\boldsymbol{r}}^e = \boldsymbol{C}_i^e (\dot{\boldsymbol{r}}^i - \boldsymbol{\Omega}_{i/e}^i \boldsymbol{r}^i) \tag{1.17}$$

Taking the second time derivative of equation (5.6) results in

$$\begin{aligned}
\ddot{\boldsymbol{r}}^e &= \boldsymbol{C}_i^e(\ddot{\boldsymbol{r}}^i - \boldsymbol{\Omega}_{i/e}^i\dot{\boldsymbol{r}}^i - \dot{\boldsymbol{\Omega}}_{i/e}^i\boldsymbol{r}^i) + \dot{\boldsymbol{C}}_i^e(\dot{\boldsymbol{r}}^i - \boldsymbol{\Omega}_{i/e}^i\boldsymbol{r}^i) \\
&= \boldsymbol{C}_i^e(\ddot{\boldsymbol{r}}^i - \boldsymbol{\Omega}_{i/e}^i\dot{\boldsymbol{r}}^i) - \boldsymbol{C}_i^e\boldsymbol{\Omega}_{i/e}^i(\dot{\boldsymbol{r}}^i - \boldsymbol{\Omega}_{i/e}^i\boldsymbol{r}^i) \\
&= \boldsymbol{C}_i^e(\ddot{\boldsymbol{r}}^i - 2\boldsymbol{\Omega}_{i/e}^i\dot{\boldsymbol{r}}^i + \boldsymbol{\Omega}_{i/e}^i\boldsymbol{\Omega}_{i/e}^i\boldsymbol{r}^i)
\end{aligned}$$

Here the Earth rotation rates are assumed to be constant. Substituting this above equation and equation (5.6) into (5.2) and (5.1) yields

Chapter 2

Strapdown Inertial Sensor Laboratory Calibration

The performance of the INS is dependent on the errors that are present in the accelerometers and gyros. The magnitude of the random errors depends on the quality of the sensor. These errors cannot be compensated for without influencing the signal itself. The repeatable errors, however, can be identified through a process called calibration and thus be compensated for. The term *sensor error* will throughout this chapter signify only a repeatable sensor error.
In this project, it is chosen to identify constant but temperature dependent errors. This is done by identifying the constant errors at various temperatures by rotating the IMU through a series of 180 rotations[Diesel, 1987]. With no translatory motion, only gravity and the rotation of the earth influences the measurements. A rotation and a measurement can be done in 5 to 20 seconds[Rogers, 2011].

2.1 Navigation Mechanization Equation

This calibration method uses a local-level navigation reference frame mechanization from which velocity errors are obtained. The navigation frame used is a geographic north-east-down (N-E-D) frame.
For this technique a simplified error dynamics model has been used[Rogers, 2011]. In this error model the earth rotation is neglected due to the short time between each rotation,

making the earth rotation very small. This simplified error model of the system is:

$$\delta\dot{v}_x = \delta f_x + g\phi_y \tag{2.1}$$
$$\delta\dot{v}_y = \delta f_y - g\phi_x \tag{2.2}$$
$$\delta\dot{v}_z = \delta f_z \tag{2.3}$$
$$\dot{\phi_x} = \Omega_z\phi_y - \Omega_y\phi_z + \epsilon_x \tag{2.4}$$
$$\dot{\phi_y} = \Omega_x\phi_z - \Omega_z\phi_x + \epsilon_y \tag{2.5}$$
$$\dot{\phi_z} = \epsilon_z \tag{2.6}$$

Where ϕ_x, ϕ_y are the misalignment angles from the sensor to the body frame around the x and y axis, δf's are the accelerometer errors whereas ϵ's represent gyro error. As the system should not be translating, any velocity is an error, so the $\dot{v}^n$ term obtained from the navigation equation (4.1) is equal to a velocity error $\delta\dot{v}^n$.
To excite all the sensor errors, the system is rotated through 3 sets of 3 rotations each.The rotations needed are shown.

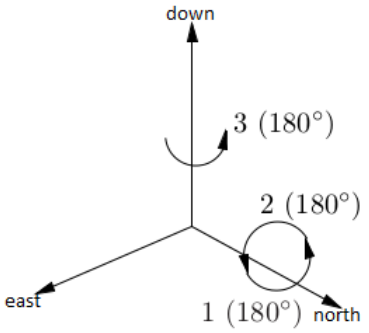

FIGURE 2.1: Rotation sequence used for calibration

2.2 Sensor error model

Accelerometer and gyro errors to be calibrated are assumed to consist of constants: bias, scale-factor, misalignment. The following equations define these contributions in the case frame(c):

$$\begin{bmatrix} \delta f_x^c \\ \delta f_y^c \\ \delta f_z^c \end{bmatrix} = \begin{bmatrix} aB_x \\ aB_y \\ aB_z \end{bmatrix} + \begin{bmatrix} aSF_x & aMA_{xy} & aMA_{xz} \\ aMA_{yx} & aSF_y & aMA_{yz} \\ aMA_{zx} & aMA_{zy} & aSF_z \end{bmatrix} \begin{bmatrix} f_x^c \\ f_y^c \\ f_z^C \end{bmatrix} \tag{2.7}$$

$$\begin{bmatrix} \varepsilon_x^c \\ \varepsilon_y^c \\ \varepsilon_z^C \end{bmatrix} = \begin{bmatrix} gB_x \\ gB_y \\ gB_z \end{bmatrix} + \begin{bmatrix} gSF_x & gMA_{xy} & gMA_{xz} \\ gMA_{yx} & gSF_y & gMA_{yz} \\ gMA_{zx} & gMA_{zy} & gSF_z \end{bmatrix} \begin{bmatrix} \omega_x^c \\ \omega_y^c \\ \omega_z^c \end{bmatrix} \tag{2.8}$$

2.3 Solution for Sensor Errors

The difference between the two horizontal velocity error components' rates of change, rotating from an initial orientation at t=0 to the final orientation at t=T is given as

$$\delta\dot{v}_x(T) - \delta\dot{v}_x(0) = \Delta\delta f_x + g\Delta\phi_y \tag{2.9}$$

$$\delta\dot{v}_y(T) - \delta\dot{v}_y(0) = \Delta\delta f_y + g\Delta\phi_x \tag{2.10}$$

where

$$\begin{aligned} \Delta\delta\boldsymbol{f} = \boldsymbol{C}_c^R(T) & \left(\begin{bmatrix} aB_x \\ aB_y \\ aB_z \end{bmatrix} + \begin{bmatrix} aSF_x & aMA_{xy} & aMA_{xz} \\ aMA_{yx} & aSF_y & aMA_{yz} \\ aMA_{zx} & aMA_{zy} & aSF_z \end{bmatrix} \begin{bmatrix} f_x^c(T) \\ f_y^c(T) \\ f_z^C(T) \end{bmatrix} \right) \\ - \boldsymbol{C}_c^R(0) & \left(\begin{bmatrix} aB_x \\ aB_y \\ aB_z \end{bmatrix} + \begin{bmatrix} aSF_x & aMA_{xy} & aMA_{xz} \\ aMA_{yx} & aSF_y & aMA_{yz} \\ aMA_{zx} & aMA_{zy} & aSF_z \end{bmatrix} \begin{bmatrix} f_x^c(0) \\ f_y^c(0) \\ f_z^C(0) \end{bmatrix} \right) \end{aligned} \tag{2.11}$$

and

$$\Delta\boldsymbol{\phi} = \int_0^T C_c^R(t) \begin{bmatrix} gSF_x & gMA_{xy} & gMA_{xz} \\ gMA_{yx} & gSF_y & gMA_{yz} \\ gMA_{zx} & gMA_{zy} & gSF_z \end{bmatrix} \boldsymbol{\omega}_{sensed}^T dt \tag{2.12}$$

Note:
-in eqn. (5.12) the contribution from the gyro bias has been temporarily ignored.
-earth rotation rate is assumed to be constant

Also, the higher derivatives of equation (9.1) and (9.2) are given as

$$\delta\ddot{v}_x = g\dot{\phi}_y = g(\Omega_x\phi_z - \Omega_z\phi_x + \varepsilon_y) \tag{2.13}$$

$$\delta\ddot{v}_y = -g\dot{\phi}_x = g(\Omega_z\phi_y - \Omega_y\phi_z + \varepsilon_x) \tag{2.14}$$

2.4 Data-collection Rotation Sequence

The rotation sequence force individual sensor error to contribute into different components of velocity error and its rate of change. These sequences are grouped into three sets, as mentioned earlier. For each of the three sets, the initial orientation of the sensor case is along a cardinal heading, that is, north. This initial orientation is changed for subsequent sets of rotations sequence. Shown in fig. 9.2 are the initial orientations of the sensor case. Also shown are the π rotations used for each sequence within the rotation set, starting from the initial orientation.

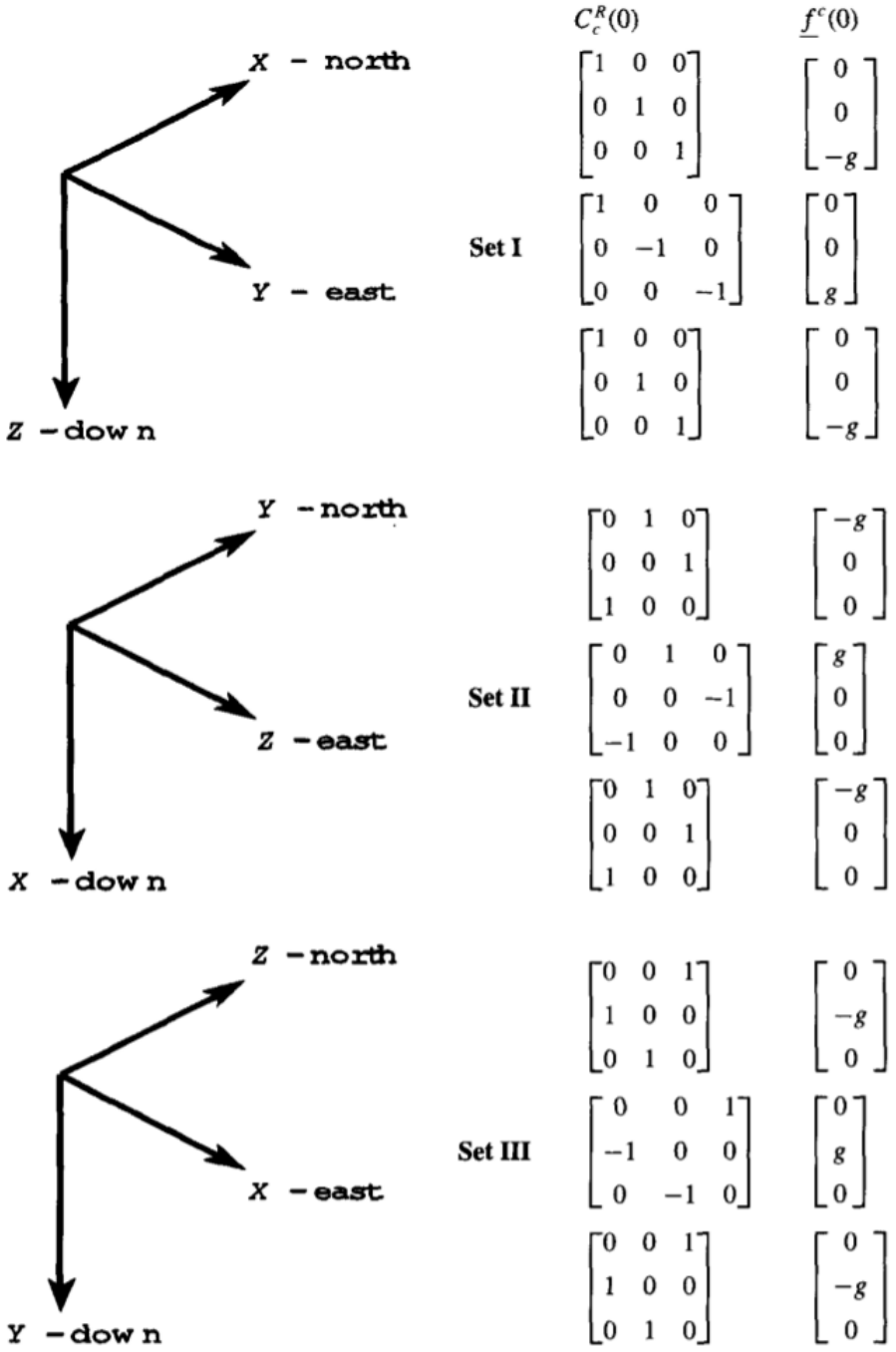

FIGURE 2.2: Rotation sets

2.5 Observation Equation

Data observed at the beginning and end of π rotations is used to extract component errors. Data set I, shown in fig. 9.2 will be used to solve for errors.

2.5.1 Rotation 1, Set 1

$$\begin{aligned}\Delta\delta\boldsymbol{f} &= \boldsymbol{C}_c^R(T)\left(\begin{bmatrix}aB_x\\aB_y\\aB_z\end{bmatrix}+g\begin{bmatrix}aMA_{xz}\\aMA_{yz}\\aSF_z\end{bmatrix}\right)-\boldsymbol{C}_c^R(0)\left(\begin{bmatrix}aB_x\\aB_y\\aB_z\end{bmatrix}-g\begin{bmatrix}aMA_{xz}\\aMA_{yz}\\aSF_z\end{bmatrix}\right)\\ &= \begin{bmatrix}2g\ aMA_{xz}\\-2aB_y\\-2aB_z\end{bmatrix}\end{aligned} \tag{2.15}$$

and

$$\begin{aligned}\Delta\boldsymbol{\phi} &= \int_0^{\pi}\begin{bmatrix}1&0&0\\0&\cos\varphi&-\sin\varphi\\0&\sin\varphi&\cos\varphi\end{bmatrix}\begin{bmatrix}gSF_x&-&-\\gMA_{yx}&-&-\\gMA_{zx}&-&-\end{bmatrix}\begin{bmatrix}\omega_x\\0\\0\end{bmatrix}dt\\ &= \int_0^{T}\begin{bmatrix}gSF_x\\gMA_{yx}\cos\varphi-gMA_{zx}\sin\varphi\\gMA_{yx}\sin\varphi+gMA_{zx}\cos\varphi\end{bmatrix}d\varphi\\ &= \begin{bmatrix}\pi gSF_x\\-2gMA_{zx}\\2gMA_{yx}\end{bmatrix}\end{aligned} \tag{2.16}$$

Substituting these results into (2.9) yields

$$\begin{aligned}\delta\dot{v}_x(T)-\delta\dot{v}_x(0) &= \Delta\delta f_x+g\Delta\phi_y\\ &= 2(aMA_{xz}-gMA_{zx})g &\equiv a_1^I\}\end{aligned} \tag{2.17}$$

Similarly for equation (2.10)

$$\begin{aligned}\delta\dot{v}_y(T)-\delta\dot{v}_y(0) &= \Delta\delta f_y+g\Delta\phi_x\\ &= -2aB_y-\pi g\ gSF_x &\{\equiv b_1^I\}\end{aligned} \tag{2.18}$$

2.5.2 Rotation 2, Set 1

$$\begin{aligned}\Delta\delta\boldsymbol{f} &= \boldsymbol{C}_c^R(T)\left(\begin{bmatrix}aB_x\\aB_y\\aB_z\end{bmatrix}-g\begin{bmatrix}aMA_{xz}\\aMA_{yz}\\aSF_z\end{bmatrix}\right)-\boldsymbol{C}_c^R(0)\left(\begin{bmatrix}aB_x\\aB_y\\aB_z\end{bmatrix}+g\begin{bmatrix}aMA_{xz}\\aMA_{yz}\\aSF_z\end{bmatrix}\right)\\ &= \begin{bmatrix}-2g\ aMA_{xz}\\2aB_y\\2aB_z\end{bmatrix}\end{aligned} \tag{2.19}$$

and

$$\begin{aligned}\Delta\boldsymbol{\phi} &= \int_0^T \begin{bmatrix} 1 & 0 & 0 \\ 0 & -\cos\varphi & \sin\varphi \\ 0 & -\sin\varphi & -\cos\varphi \end{bmatrix} \begin{bmatrix} gSF_x & - & - \\ gMA_{yx} & - & - \\ gMA_{zx} & - & - \end{bmatrix} \begin{bmatrix} \omega_x \\ 0 \\ 0 \end{bmatrix} dt \\ &= \int_0^\pi \begin{bmatrix} gSF_x \\ -gMA_{yx}\cos\varphi + gMA_{zx}\sin\varphi \\ -gMA_{yx}\sin\varphi - gMA_{zx}\cos\varphi \end{bmatrix} d\varphi \\ &= \begin{bmatrix} \pi gSF_x \\ 2gMA_{zx} \\ -2gMA_{yx} \end{bmatrix} \end{aligned} \tag{2.20}$$

Substituting these results into (2.9) yields

$$\begin{aligned}\delta\dot{v}_x(T) - \delta\dot{v}_x(0) &= \Delta\delta f_x + g\Delta\phi_y \\ &= -2(aMA_{xz} - gMA_{zx})g \qquad \{\equiv a_2^I\}\end{aligned} \tag{2.21}$$

Similarly for equation (2.10)

$$\begin{aligned}\delta\dot{v}_y(T) - \delta\dot{v}_y(0) &= \Delta\delta f_y + g\Delta\phi_x \\ &= 2aB_y - \pi g\ gSF_x \qquad \{\equiv b_2^I\}\end{aligned} \tag{2.22}$$

2.5.3 Rotation 3, set 1

$$\begin{aligned}\Delta\delta\boldsymbol{f} &= \boldsymbol{C}_c^R(T)\left(\begin{bmatrix} aB_x \\ aB_y \\ aB_z \end{bmatrix} - g\begin{bmatrix} aMA_{xz} \\ aMA_{yz} \\ aSF_z \end{bmatrix}\right) - \boldsymbol{C}_c^R(0)\left(\begin{bmatrix} aB_x \\ aB_y \\ aB_z \end{bmatrix} - g\begin{bmatrix} aMA_{xz} \\ aMA_{yz} \\ aSF_z \end{bmatrix}\right) \\ &= \begin{bmatrix} -2aB_x + 2g\ aMA_{xz} \\ -2aB_y + 2aB_y \\ 0 \end{bmatrix}\end{aligned} \tag{2.23}$$

and

$$\begin{aligned}\Delta\boldsymbol{\phi} &= \int_0^T \begin{bmatrix}\cos\psi & -\sin\psi & 0\\ \sin\psi & \cos\psi & -0\\ 0 & 0 & 1\end{bmatrix}\begin{bmatrix}- & - & gMA_{xz}\\ - & - & gMA_{yz}\\ - & -gSF_z & \end{bmatrix}\begin{bmatrix}0\\0\\\omega_z\end{bmatrix} dt\\ &= \int_0^\pi \begin{bmatrix} \\ gMA_{xz}\cos\psi - gMA_{yz}\sin\psi\\ gMA_{xz}\sin\psi + gMA_{yz}\cos\psi\\ gSF_z\end{bmatrix} d\varphi\\ &= \begin{bmatrix}-2sMA_{yz}\\ 2gMA_{xz}\\ \pi gSF_z\end{bmatrix}\end{aligned} \tag{2.24}$$

Substituting these results into (2.9) yields

$$\begin{aligned}\delta\dot{v}_x(T) - \delta\dot{v}_x(0) &= \Delta\delta f_x + g\Delta\phi_y\\ &= -2aB_x + 2(aMA_{xz} + gMA_{xz})g \qquad \{\equiv a_3^I\}\end{aligned} \tag{2.25}$$

Similarly for equation (2.10)

$$\begin{aligned}\delta\dot{v}_y(T) - \delta\dot{v}_y(0) &= \Delta\delta f_y + g\Delta\phi_x\\ &= -2aB_y + 2(aMA_{yz} + gMA_{yz})g \qquad \{\equiv b_3^I\}\end{aligned} \tag{2.26}$$

Continuing with rotation sequence 3, Eqns. (2.13-2.14) are applied to data at the beginning and end of this rotation. This additional computation permits the tilt errors ϕ_x and ϕ_y, and the azimuth error ϕ_z, to be expressed in terms of the velocity error rate-of-change as

$$\begin{aligned}\delta\ddot{v}_x(T) - \delta\ddot{v}_x(0) &= g(-gB_y + \Omega_x\phi_z - \Omega_z\phi_x) - g(gB_y + \Omega_x\phi_z - \Omega_z\phi_x)\\ &= -2g\ gB_y\end{aligned} \tag{2.27}$$

$$\begin{aligned}\delta\ddot{v}_y(T) - \delta\ddot{v}_y(0) &= g(-gB_x + \Omega_z\phi_y - \Omega_y\phi_z)gg(gB_x + \Omega_z\phi_y - \Omega_y\phi_z)\\ &= -2g\ gB_x\end{aligned} \tag{2.28}$$

and

$$\begin{aligned}\delta\ddot{v}_y(T) + \delta\ddot{v}_y(0) &= g(-gB_y + \Omega_x\phi_z - \Omega_z\phi_x) + g(gB_y + \Omega_x\phi_z - \Omega_z\phi_x)\\ &= -2g\Omega_z\phi_x + 2g\Omega_x\phi_z\end{aligned} \tag{2.29}$$

From eqns. (9.1) and (9.2) we get

$$\begin{aligned} \delta\dot{v}_x(T) + \delta\dot{v}_x(0) &= -\delta f_x + g\phi_y + (\delta f_x + g\phi_y) \\ &= 2g\phi_y \end{aligned} \tag{2.30}$$

$$\begin{aligned} \delta\dot{v}_y(T) + \delta\dot{v}_y(0) &= -\delta f_y - g\phi_x + (\delta f_y - g\phi_x) \\ &= 2g\phi_x \end{aligned} \tag{2.31}$$

The errors for Set II and Set III can be obtained from those of set I by permuting the subscripts. Solution for all the errors is summarized is Table 2.2. Also Table 2.1 lists the measurements of the rate-of-change of velocity errors. These measurements are done just before and after the π rotations.

Table 9.1 Observation equations for errors

	Set I	Set II	Set III
Rotation 1	$a_1^I \equiv 2(aMA_{xz} - gMA_{zx})g$	$a_1^{II} \equiv 2(aMA_{yx} - gMA_{xy})g$	$a_1^{III} \equiv 2(aMA_{zy} - gMA_{yz})g$
	$b_1^I \equiv -2\,aB_y - \pi g\, gSF_x$	$b_1^{II} \equiv -2\,aB_z - \pi g\, gSF_y$	$b_1^{III} \equiv -2\,aB_x - \pi g\, gSF_z$
Rotation 2	$a_2^I \equiv -2(aMA_{xz} - gMA_{zx})g$	$a_2^{II} \equiv -2(aMA_{yx} - gMA_{xy})g$	$a_2^{III} \equiv -2(aMA_{zy} - gMA_{yz})g$
	$b_2^I \equiv 2\,aB_y - \pi g\, gSF_x$	$b_2^{II} \equiv 2\,aB_z - \pi g\, gSF_y$	$b_2^{III} \equiv 2\,aB_x - \pi g\, gSF_z$
Rotation 3	$a_3^I \equiv -2\,aB_x + 2(aMA_{xz} + gMA_{xz})g$	$a_3^{II} \equiv -2\,aB_y + 2(aMA_{yx} + gMA_{yx})g$	$a_3^{III} \equiv -2\,aB_z + 2(aMA_{zy} + gMA_{zy})g$
	$b_3^I \equiv -2\,aB_y + 2(aMA_{yz} + gMA_{yz})g$	$b_3^{II} \equiv -2\,aB_z + 2(aMA_{zx} + gMA_{zx})g$	$b_3^{III} \equiv -2\,aB_x + 2(aMA_{xy} + gMA_{xy})g$

Table 9.2 Solution for errors

	Set I	Set II	Set III
Gyro scale factor	$gSF_x = \dfrac{b_2^I + b_1^I}{-2\pi g}$	$gSF_y = \dfrac{b_2^{II} + b_1^{II}}{-2\pi g}$	$gSF_z = \dfrac{b_2^{III} + b_1^{III}}{-2\pi g}$
Accel bias	$aB_y = \dfrac{b_2^I - b_1^I}{4}$	$aB_z = \dfrac{b_2^{II} - b_1^{II}}{4}$	$aB_x = \dfrac{b_2^{III} - b_1^{III}}{4}$
Axis definition	$aMA_{xz} \equiv 0 \,\&\, aMA_{yz} \equiv 0$	$aMA_{yx} \equiv 0$	
Gyro misalignment	$gMA_{yz} = \dfrac{b_3^I + 2\,aB_y}{2g}$	$gMA_{yx} = \dfrac{a_3^{II} + 2\,aB_y}{2g}$	$gMA_{zy} = \dfrac{b_3^{III} + 2\,aB_z}{2g} - aMA_{zy}$
	$gMA_{zx} = \dfrac{a_1^I}{-2g}$	$gMA_{xy} = \dfrac{a_1^{II}}{-2g}$	
	$gMA_{xz} = \dfrac{a_3^I + 2\,aMA_x}{2g}$		
Accel misalignment		$aMA_{zx} = \dfrac{b_3^{II} + 2\,aMA_z}{2g} - gMA_{zx}$	$aMA_{xy} = \dfrac{b_3^{III} + 2\,aB_x}{2g} - gMA_{xy}$
			$aMA_{zy} = \dfrac{a_1^{III}}{2g} + gMA_{yz}$

2.6 Simulation

Simulation was carried out, using the developed error equations, to generate the data for the inertial navigation sensor. In the simulation the navigation equations are implemented in a local-level N-E-D frame. The sensor errors included are the accelerometer and gyro biases and scaling-factor[Diesel,1987].
Note that the process assumes the availability of rate-of-change of velocity errors. This availability is satisfied by using a tracking model, implemented in a Kalman filter algorithm, to produce estimates of the rate of change of velocity errors. The tracking filter dynamics model is

$$\frac{d}{dt}\begin{bmatrix}\delta v_i \\ \dot{\delta} v_i \\ \ddot{\delta} v_i\end{bmatrix} = \begin{bmatrix}0 & 1 & 0 \\ 0 & 0 & 1 \\ 0 & 0 & 0\end{bmatrix}\begin{bmatrix}\delta v_i \\ \dot{\delta} v_i \\ \ddot{\delta} v_i\end{bmatrix} + \begin{bmatrix}0 \\ 0 \\ w_i\end{bmatrix} \tag{2.32}$$

and measurement matrix

$$y = \boldsymbol{h}\begin{bmatrix}\delta v_i \\ \dot{\delta} v_i \\ \ddot{\delta} v_i\end{bmatrix} \tag{2.33}$$

where

$$\boldsymbol{h} = \begin{bmatrix}1 & 0 & 0\end{bmatrix}$$

$$w_r = measurementnoise$$

2.6.1 Results

The 3-axis turn table on which the inertial sensors are mounted is given the following control input.

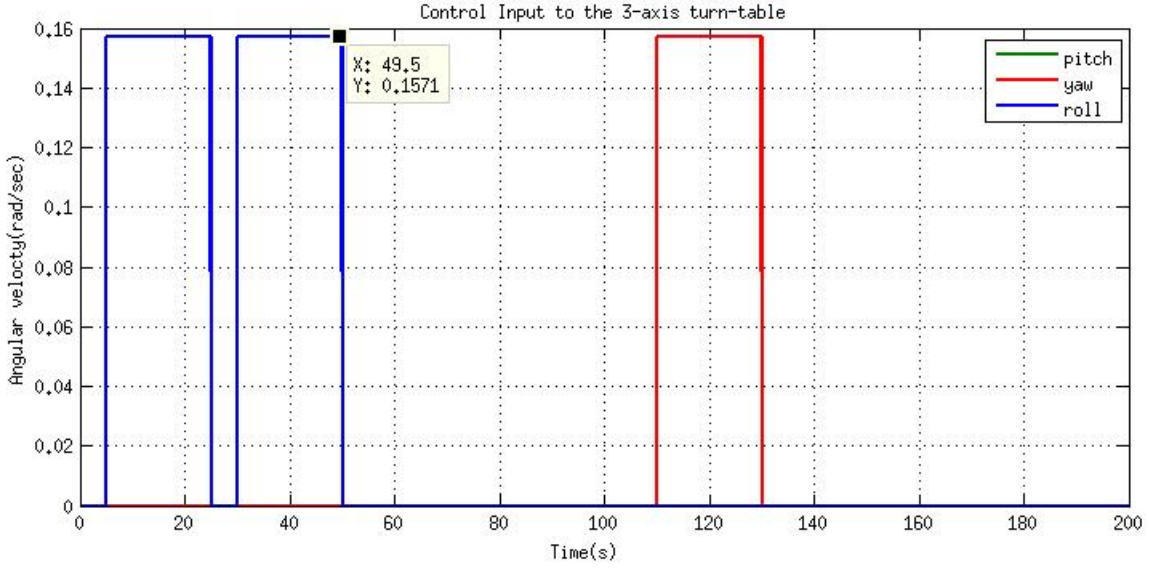

FIGURE 2.3: Input to turn table, for π rotations.

The navigation frame is subjected to only a pure rotational motion. And therefore the translational velocities $\{ v_n \; v_e \; v_d \}$ must be zero. This is indeed the case when the ideal inertial sensors, i.e. without any bias, scale-factor or misalignment error are modelled.

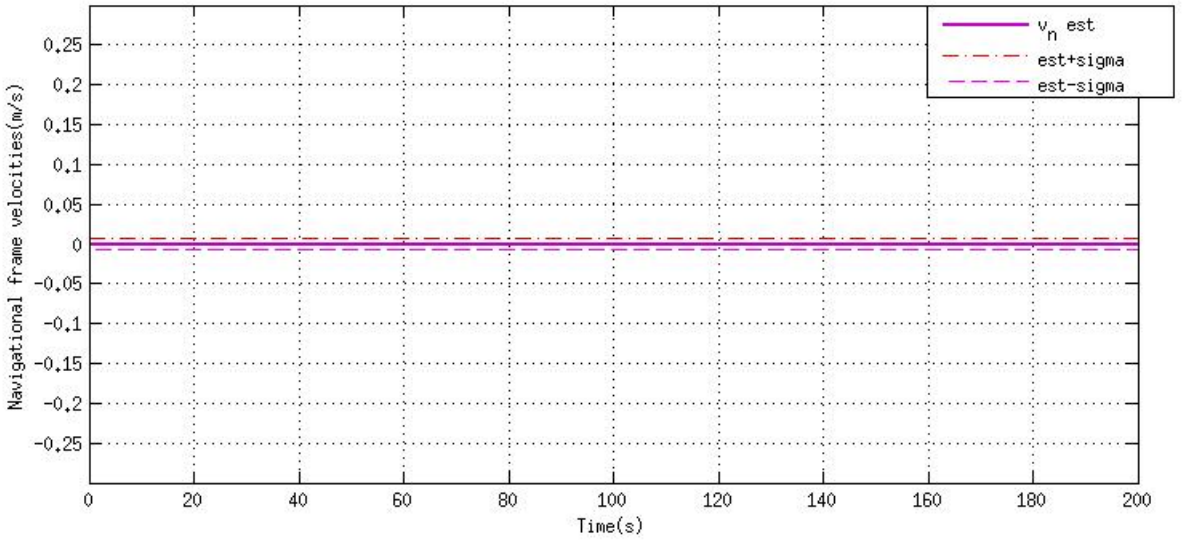

FIGURE 2.4: Simulated ideal inertial sensor north velocity filter estimate

Now, the actual sensor model being used in the simulation is[Diesel, 1987] Gyro model:

$$\begin{aligned} x &: (1 - 0.003805)u_x + 1.443 * 10^{-5} \\ y &: (1 - 0.003805)u_y + 8.941 * 10^{-5} \\ z &: (1 - 0.00144)u_z + 1.589 * 10^{-5} \end{aligned}$$

Accelerometer model:

$$\begin{aligned} x &: (1 - 0.000785)u_x + 0.371 \\ y &: (1 - 0.000785)u_y + 0.2298 \\ z &: (1 - 0.003283)u_z + 0.1711 \end{aligned}$$

Using this in the simulation model we obtain the following characteristic of the rate-of-change of error in east-velocity v_e

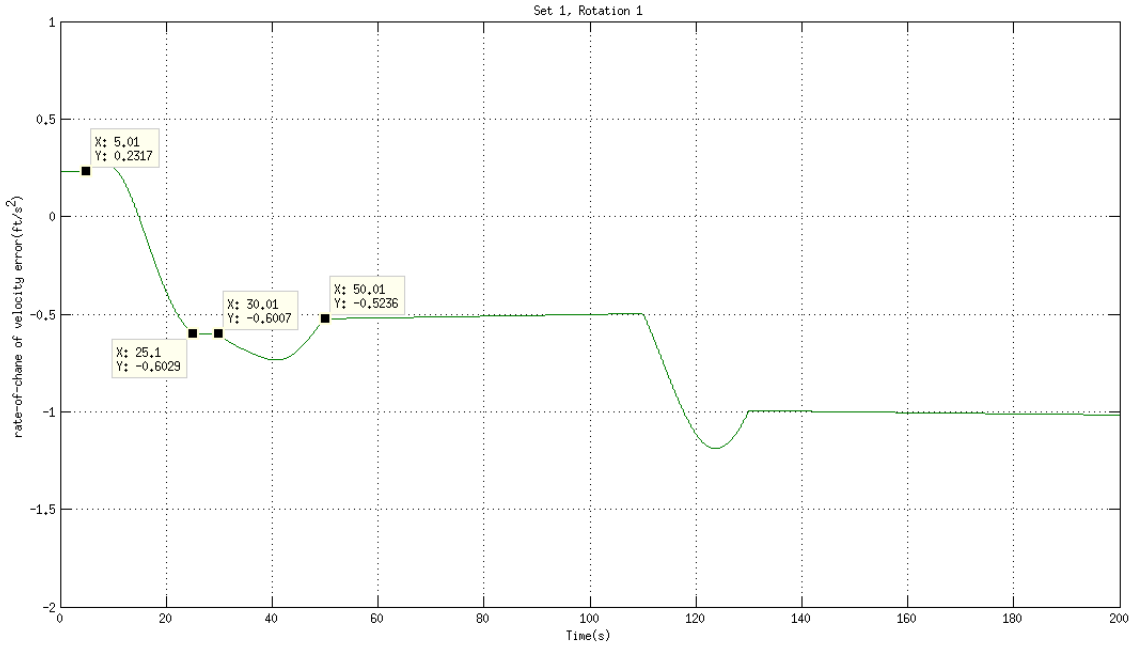

FIGURE 2.5: Simulated ideal inertial sensor north velocity filter estimate

As mentioned earlier, readings are taken right before and after the rotation of the turn-table. Using this information and relations from table (2.2) we calculate

$$gSF_x = \frac{b_2^I + b_1^I}{2\pi g} = -0.0038 \quad (2.34)$$

$$aB_y = \frac{b_2^I - b_1^I}{4} = 0.2279 \quad (2.35)$$

Chapter 3

Inertial Navigation with Aiding

Unaided Inertial sensors based navigation inevitably suffer from unbounded errors in velocity, position and attitude. This is unacceptable in many applications. For this reason some kind of aiding is needed to either bound or reduce these errors. Many different forms of aiding can be used giving various results. Some of the more popular aiding devices are Global Positioning System (GPS) and barometric measurements. The main idea is that, with independent information at hand, both the sensors are able to estimate the navigation state vector(position, velocity, attitude) with greater accuracy.

3.1 Motivation for GPS/INS integration

One of the most important advantages of inertial navigators is that they require no interaction with the environment beyond the user. Contrast this with GPS, which inherently relies upon signals transmitted from satellites. These signals can be jammed or be unavailable owing to the environment of operation(eg. underwater/indoors etc.), rendering the navigational aid useless.
In terms of data rates, the rate of computation of navigational states in an inertial navigator is restricted only by the processing power available in the host computer. Some INS are capable of generating estimates of the navigational state-vector at 100Hz or more. In contrast most GPS receivers have data rates of the order of 1-20Hz[Gleason,].
GPS and INS are complementary in terms of the information they provide. Strictly speaking, though GPS can provide attitude solution, but its avoided as its quite complex(multiple receivers and antennas) and potentially costly. Whereas, attitude is a necessary output of the INS algorithm.
Finally, and most importantly, GPS and INS both have complementary error characteristics. The INS output errors are time-correlated and unbound(especially with low-cost

sensors). A GPS receiver, on the other hand, generates position and velocity estimates with bound errors.

3.2 Global Position System

GPS receiver uses a one-way ranging technique from the GPS satellites that are also broadcasting their estimated positions. Signals from four satellites are used with the user generated replica signal and the relative phase is measured. Using triangulation the location of the receiver is fixed. Four unknowns can be determined using the four satellites and appropriate geometry : (a.)latitude, (b.)longitude, (c.)altitude and (d.)a correction to the user's clock.
The GPS ranging signal is broadcast at two frequencies : a primary signal at 1575.42 MHz (L_1) and a secondary broadcast at 1227.6 MHz (L^2). Civilians use the L_1 frequency, which has two modulations, namely ***C/A*** (Clear/Coarse Acquisition) Code and ***P*** (Precise/Protected) Code. C/A is unencrypted signal broadcast at a higher bandwidth and is available only on L_1 . P code is more precise because it is broadcast at a higher bandwidth and is restricted for military use. The military operators can degrade the accuracy of the C/A code intentionally and this is known as Selective Availability. Ranging errors of the order of 100m can exist with Selective Availability[Gleason]. There are six major causes of ranging errors :(a.)satellite ephemeris broadcast error, (b.)satellite clock errors, (c.)ionospheric group delay, (d.)tropospheric group delay, (e.)multi path and (f.)receiver measurement errors, including software.
Ionospheric and Tropospheric errors can be eliminated by using carrier phase measurements and/or DGPS. Further, the satellite geometry too has an effect on the accuracy of the measurement. The error due satellite geometry is quantified by the parameter called Geometric Dilution of Precision (GDOP). The farther away the satellites, the smaller (and the better) the value of GDOP will be. A satellite configuration GDOP value of less than 5 is considered as a good geometry.

3.3 GPS-INS Integration Architectures

There are various ways of fusing the GPS and INS measurements together, so that we have a relatively more accurate navigator than either of standalone GPS or INS based one. The crudest form of integration is to obtain a solution from GPS of position and velocity estimates so as to reinitialize the inertial navigation equations. In this case the equations of GPS and INS are totally uncoupled, but as soon as the INS errors grow out

of bounds, the errors are brought back to the accuracy provided by the GPS.
The variation in integration architectures lies in mainly three fields:

- The way in which INS errors are corrected by GPS measurements
- The type of GPS measurement being used
- The way in which GPS receiver is aided by the INS

Also, depending upon whether the correction is applied to reinitialize the INS after every time-step, or whether the INS is not reset, we have open(feed-forward; generally used with high quality INS such as those in commercial aircrafts) and close loop(feedback) architectures.
Keeping in mind the above pointers, the various GPS-INS integration approaches are defined as:
1)*Loosely Coupled*

- GPS position and velocity solution is used for aiding
- Involves cascaded Kalman Filters, the first PV EKF for GPS and then the integrated Kalman Filter
- Is the simplest type of architecture, usually used while retrofitting the GPS in existing systems with INS

2)*Tightly Coupled*

- INS and GPS are reduced to their basic sensor functions, i.e. pseudorange (ρ), $\dot{\rho}$ and accelerometer, gyro measurements
- These measurements are used to generate single blended navigation solution.
- Both the Kalman Filter are in a way joint into one, hence, only a single Kalman Filter is required in this type of architecture
- This architecture doesn't require a full fix of position and velocity from the GPS, thus making it more robust

3)*Deeply Coupled*

- This is an advanced architecture involving deep integration of INS and GPS

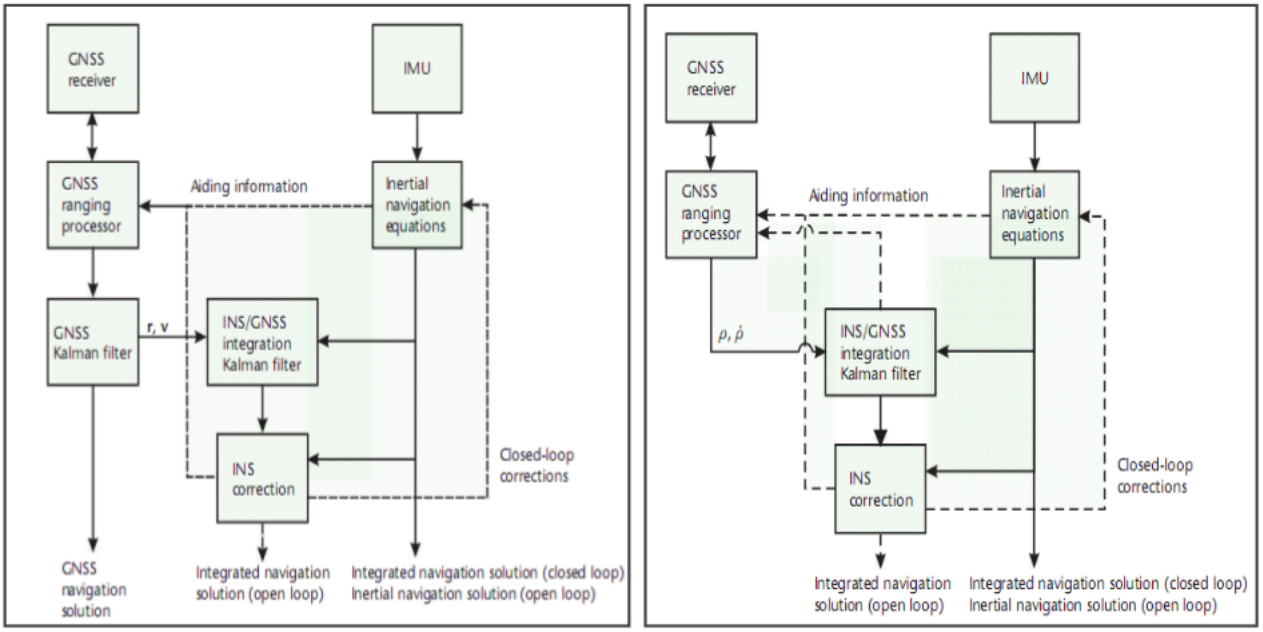

FIGURE 3.1: Loosely Coupled and Tightly Coupled Approaches (Source:Groves,2008)

- It combines GPS Navigation and Tracking. Information from the INS is used to track the satellites
- This also uses a single Kalman Filter wherein all the states required for GPS-INS integration and Satellite tracking are estimated

The INS configuration Kalman Filter we;ll study is that of an open loop architecture, as the navigation corrections are not used to reset the INS propagation equations. Moreover, it can be said to be a tightly coupled configuration since pseudorange measurements are being used and a combined EKF finds out the navigation solution.

3.4 INS-configuration Kalman Filter

This section describes an open loop tightly coupled GPS - INS architecture, the author of Ref. [9; Rogers] however refers to it as an INS Configuration Kalman Filter. It is a 12state EKF which uses GPS measurements to obtain estimates of error states of position, velocity and platform tilt.

3.4.1 True Motion

The aircraft motion is simulated using navigation equation in the N-E-D Frame. The aircraft initiates at

- Latitude = 18.92 degrees
- Longitude = 72.90 degrees
- Altitude =5000 ft.(doesn't effect the simulations in the absence of an aircraft dynamics model)
- Velocity in East direction = 650 km/h
- Velocity in North and Down Direction = 0

The aircraft motion is governed by the bank command, and the aircraft is following the bank-to-turn manoeuvre. The environment model (which can be replaced by data from

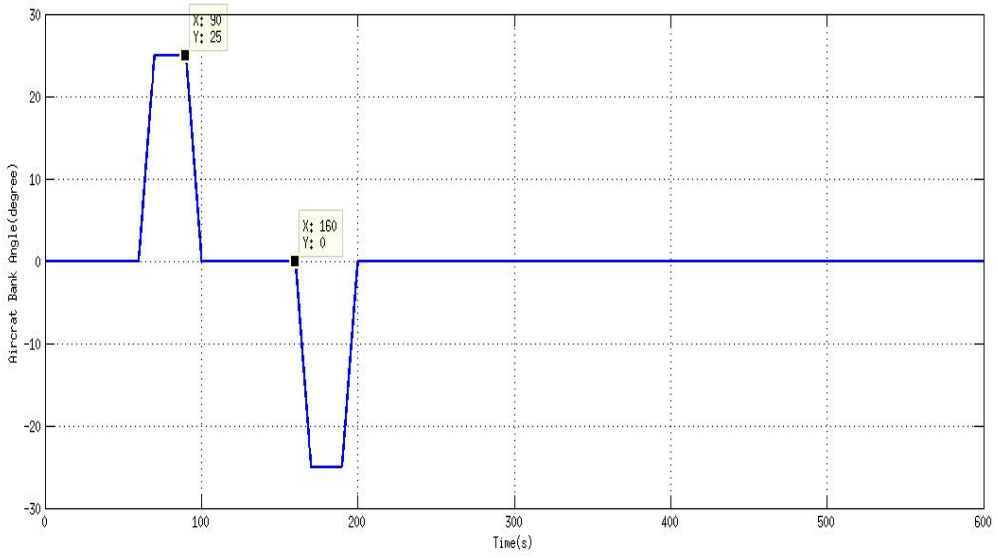

FIGURE 3.2: Aircraft Bank Angle INS-EKF

a real flight) gives the true value of

- Latitude, Longitude and Altitude of the Aircraft
- Velocity in NED Frame
- Transformation Matrix from Body to NED Frame, C_{bv}
- Inertial Angular Velocity of the aircraft expressed in Body Frame, $\omega^b_{i/b}$; which is measured by the gyros.
- Acceleration with respect to NED frame expressed in Body Frame, f_b

The bank angle is denoted by η then rate of turn which contributes to the body rate is:

$$Rate\ of\ turn = gtan(\eta)/|V|$$

The acceleration in the navigation frame is obtained by the following expression and then is converted to the body frame of reference,

$$\begin{aligned} f_g &= \dot{v}_g + (\Omega^g_{e/g} + 2\Omega i/e^g)v_g - g_g \\ f_b &= C_{bg} f_g \end{aligned}$$

The attitude dynamics of the aircraft is described by:

$$\dot{C}_{bn} = \Omega^b_{n/b} C_{bn}$$

Lastly, the propagation of latitude, longitude and altitude is given by:

$$\begin{aligned} \dot{\lambda} &= \frac{V_N}{R+h} \\ \dot{\varphi} &= \frac{V_E}{(R+h)\cos(\lambda)} \\ \dot{h} &= -V_D \end{aligned}$$

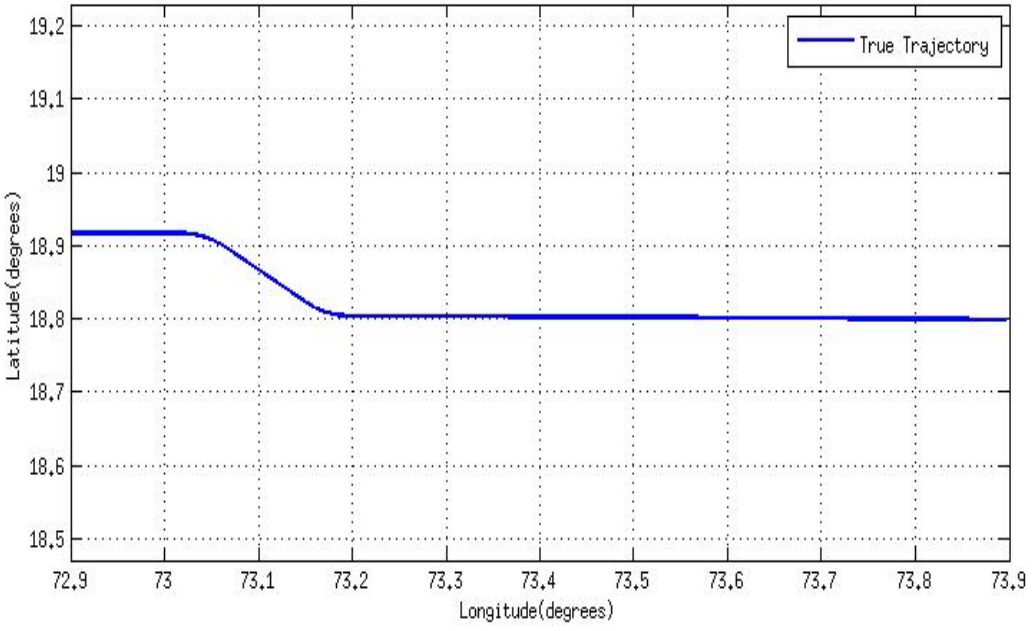

FIGURE 3.3: True Aircraft Trajectory (INS EKF)

3.4.2 Sensor Models

1)Gyro

- measures $\omega^b_{i/b}$, Inertial Body Rate expressed in Body Frame
- Gyro errors were described earlier, for our problem we have considered the gyro to have bias and white noise
- Bias = 0.1 degree/hour [Rogers]
- White Noise Power Spectral Density(PSD) = $2.35 * 10^{-11}$ w/kg/Hz [Bar-Shalom]

2)Accelerometer

- It measures acceleration of the aircraft in navigation frame expressed in body frame, f_B
- Accelerometer is also modelled to have bias and white noise
- Bias = 0.01g [Rogers]
- White Noise PSD = 0.0036 w/kg/Hz [Bar-Shalom]

3)GPS Receiver

- GPS Noise is approximated as exponentially auto-correlated noise

The GPS receiver clock is modelled using two state components, clock bias b and clock drift d. The governing equations for the clock bias are given as:

$$\begin{aligned} \dot{b}(t) &= d(t) + \bar{v}_b(t) \\ \dot{d}(t) &= \bar{v}(t) \end{aligned}$$

In discrete time form,

$$\begin{aligned} x_c(k+1) &= F_2 x_c(k) + v_c(k) \\ F_2 &= \begin{bmatrix} 1 & T \\ 0 & 1 \end{bmatrix} \end{aligned}$$

where x_c=$c[bd]^T$ and $v_c(k)$ has zero mean and the following covariance matrix

$$Q_c = S_b T c^2 \begin{bmatrix} 1 & 0 \\ 0 & 0 \end{bmatrix} + S_d c^2 \begin{bmatrix} \frac{T^3}{3} & \frac{T^2}{2} \\ \frac{T^2}{2} & T \end{bmatrix}$$

The parameters S_b, S_d are the noise parameters for a clock, and there mean value depends upon the type of the clock. For crystal clocks the typical values are of the order of $4x10^{-20}$ and $8x10^{-19}$, respectively.
Apart from the above mentioned sensors, altimeter is also simulated in some cases. The GPS-INS Kalman filter can work without altimeter, however since the altimeter makes the vertical channel stable, it reduces the rate of growth of error.

3.4.3 INS - Configuration Filter

The configuration EKF also resides on the Flight Computer and integrates the data from the INS and GPS to give refined estimates of navigation error. The EKF consists of 12 states namely

- Position Error Vector in Navigation Frame 3 States
- Velocity Error Vector in Navigation Frame 3 States
- INS platform attitude error vector 3 States
- Altimeter Bias 1 State
- GPS Receiver Clock Bias 1 State (clock error*speed of light)
- GPS Receiver Clock Drift 1 State

The state space equation governing the above states (Process Model) is given by,

$$\dot{x}(t) = A(t)x(t) + v(t) \tag{3.1}$$

where v(t) denotes the random white noise in the process.
The A matrix (continuous time) is obtained from governing equations of each of the state variables, described in previous sections. where $\rho = \omega^n_{e/n}$ $\Omega = \omega^n_{i/e}$.
To obtain the discrete time version of the A(t) matrix we use the approximation

$$F(k) = I + A(t)xT$$

The Process Noise Covariance Matrix used in our simulations is given as follows:

$$Q_{1:10} = diag(11110^{-3}10^{-3}10^{-3}10^{-12}10^{-12}10^{-12}10)xT \tag{3.2}$$

$$Q_{11:12} = Q_c \tag{3.3}$$

$$A(t) = \begin{bmatrix}
0 & 0 & -\rho_y & 1 & 0 & 0 & 0 & 0 & 0 & 0 & 0 & 0 \\
0 & 0 & \rho_x & 0 & 1 & 0 & 0 & 0 & 0 & 0 & 0 & 0 \\
\rho_y & -\rho_x & 0 & 0 & 0 & 1 & 0 & 0 & 0 & 0 & 0 & 0 \\
\frac{f_z - g}{R} & 0 & 0 & 0 & 2\Omega_z & -\left(\rho_y + 2\Omega_y\right) & 0 & -f_z & f_y & 0 & 0 & 0 \\
0 & \frac{f_z - g}{R} & 0 & -2\Omega_z & -\frac{v_z}{R} & (\rho_x + 2\Omega_x) & f_z & 0 & -f_x & 0 & 0 & 0 \\
-\frac{f_x}{R} & -\frac{f_y}{R} & \frac{2g}{R} & \left(\rho_y + 2\Omega_y\right) & -(\rho_x + 2\Omega_x) & 0 & -f_y & f_x & 0 & 0 & 0 & 0 \\
0 & 0 & 0 & 0 & 0 & 0 & 0 & \Omega_z & -\left(\rho_y + \Omega_y\right) & 0 & 0 & 0 \\
0 & 0 & 0 & 0 & 0 & 0 & -\Omega_z & 0 & \left(\rho_x + \Omega_x\right) & 0 & 0 & 0 \\
0 & 0 & 0 & 0 & 0 & 0 & \left(\rho_y + \Omega_y\right) & -\left(\rho_x + \Omega_x\right) & 0 & 0 & 0 & 0 \\
0 & 0 & 0 & 0 & 0 & 0 & 0 & 0 & 0 & \frac{-1}{\tau_h} & 0 & 0 \\
0 & 0 & 0 & 0 & 0 & 0 & 0 & 0 & 0 & 0 & 0 & 1 \\
0 & 0 & 0 & 0 & 0 & 0 & 0 & 0 & 0 & 0 & 0 & 0
\end{bmatrix}$$

The diagonal elements represent the covariance in respective state, i.e. the first three components represent covariance of 1 m2/s in the process noise, the next three component represent covariance of 10 -3 m2/s3 in lateral direction and of 10-3 m2/s3 in vertical channel. Similarly, rest of the components represent covariance of process noise of the respective state. By combining the two matrices Q1:10 and Qc we obtain the whole process noise covariance.

$$Q = \begin{bmatrix} Q_{1:10} & Q_{10x2} \\ Q_{2x10} & Q_{11:12} \end{bmatrix}$$

3.5 Simulation Results

Bibliography

[] A. S. Arnold, J. S. Wilson, and M. G. Boshier. A simple extended-cavity diode laser. *Review of Scientific Instruments*, 69(3):1236–1239, March 1998. URL http://link.aip.org/link/?RSI/69/1236/1.

[] Carl E. Wieman and Leo Hollberg. Using diode lasers for atomic physics. *Review of Scientific Instruments*, 62(1):1–20, January 1991. URL http://link.aip.org/link/?RSI/62/1/1.

[] C. J. Hawthorn, K. P. Weber, and R. E. Scholten. Littrow configuration tunable external cavity diode laser with fixed direction output beam. *Review of Scientific Instruments*, 72(12):4477–4479, December 2001. URL http://link.aip.org/link/?RSI/72/4477/1.